Prognostic significance of liver CT-attenuation and ^{18}F-FDG uptake for predicting hepatic recurrence following curative resection of colorectal cancer

Jeong Won Lee[1] MD, PhD,
Hyein Ahn[2] MD, PhD,
Su Jin Jang[3] MD, PhD,
Moo-Jun Baek[4] MD, PhD,
Nam Hun Heo[5] MS,
Sang Mi Lee[6] MD, PhD

1. Department of Nuclear Medicine, Catholic Kwandong University College of Medicine, International St. Mary's Hospital, Incheon, Korea
2. Department of Pathology, Soonchunhyang University Cheonan Hospital, Cheonan, Korea
3. Department of Nuclear Medicine, CHA Bundang Medical Center, CHA University, Seongnam-si, Korea
4. Department of Surgery, Soonchunhyang University Cheonan Hospital, Cheonan, Korea
5. Clinical Trial Center, Soonchunhyang University Cheonan Hospital, Cheonan, Korea
6. Department of Nuclear Medicine, Soonchunhyang University Cheonan Hospital, Cheonan, Korea

Keywords: Colorectal cancer - ^{18}F-FDG - Liver metastasis - PET/CT - Prognosis

Corresponding author:
Sang Mi Lee, MD, PhD
Soonchunhyang University Cheonan Hospital,
31 Suncheonhyang 6-gil,
Dongnam-gu, Cheonan,
Chungcheongnam-do, 31151,
Republic of Korea
Telephone: +82-41-570-3540
Fax: +82-41-572-4655
gareen@naver.com

Received:
17 January 2022
Accepted revised:
2 August 2022

Abstract

Objective: This study investigated the predictive values of computed tomography (CT)-attenuation and fluorine-18-fluorodeoxyglucose (^{18}F-FDG) uptake in the liver for the hepatic recurrence of colorectal cancer. **Subjects and Methods:** This study retrospectively included 257 colorectal cancer patients who underwent staging ^{18}F-FDG positron emission tomography (PET)/CT and were subsequently treated with curative surgical resection. Using noncontrast-enhanced CT images in PET/CT, the liver-spleen ratio and liver-spleen difference of CT-attenuation and CT-attenuation of the liver were calculated. The maximum and mean ^{18}F-FDG uptake in the liver was measured using the PET images. The relationship of these five liver parameters to recurrence-free survival (RFS), hepatic RFS, and extrahepatic RFS was assessed. **Results:** In univariate survival analysis, the liver-spleen ratio, liver-spleen difference, and maximum ^{18}F-FDG uptake of the liver were significant predictors of both RFS and hepatic RFS ($P<0.05$), whereas none of the five liver parameters were significantly associated with extrahepatic RFS ($P>0.05$). Patients with a low liver-spleen ratio and liver-spleen difference and a high maximum ^{18}F-FDG uptake showed better hepatic RFS than those with a high liver-spleen ratio and liver-spleen difference and a low maximum ^{18}F-FDG uptake. In multivariate analysis, the liver-spleen ratio, liver-spleen difference, and maximum ^{18}F-FDG uptake of liver remained significant predictors for hepatic RFS after adjusting for age, sex, obesity, and stage ($P<0.05$). **Conclusions:** Computed tomography-attenuation and maximum ^{18}F-FDG uptake in the liver on ^{18}F-FDG PET/CT were significant predictive factors for hepatic RFS in patients with colorectal cancer after curative resection.

Hell J Nucl Med 2022; 25(2): 177-187 *Published online: 29 August 2022*

Introduction

The liver is the most common organ of the distant metastasis of colorectal cancer, and approximately 13%-30% of the patients with colorectal cancer experience hepatic metastasis after the diagnosis of colorectal cancer (metachronous hepatic metastasis) [1, 2]. In colorectal cancer patients with hepatic metastasis, the progression of hepatic metastasis rather than the progression of the primary tumor lesion mainly determines overall survival, and most patients die within three years after the diagnosis [1, 3, 4]. One of the potential curative therapy for metachronous hepatic metastasis is the surgical resection of metastatic lesions [2]. However, only 25% of the colorectal cancer patients with hepatic metastasis are eligible for surgical resection, and even when hepatic resection is performed, the five-year overall survival rates are still low at 38%-50% with a recurrence rate of 60% [5, 6]. Therefore, a number of studies have been performed to investigate the predictive factors for metachronous hepatic metastasis in patients with colorectal cancer. In addition to the well-known tumor intrinsic factors such as the tumor-node-metastasis (TNM) stage and serum carcinoembryonic antigen (CEA), several recent studies also focused on the significance of the liver microenvironment in the formation and growth of hepatic metastasis [7-10], since the microenvironment of the target tissue plays a critical role in the success of cancer cell metastasis [11]. In previous studies, fatty changes and inflammatory conditions in the liver were found to be associated with the occurrence of hepatic metastasis in patients with colorectal cancer; however, inconsistent results have been reported, showing both positive and negative associations [7-10].

Fluorine-18-fluorodeoxyglucose (^{18}F-FDG) positron emission tomography/computed tomography (PET/CT) is currently used for staging work-up, assessing tumor biological characteristics, and predicting prognosis in patients with colorectal cancer [12, 13]. Considering that the CT-attenuation of noncontrast-enhanced CT images is used for evaluating fatty changes in the liver and the degree of ^{18}F-FDG uptake in the liver is considered

to be related to inflammatory condition in the liver [14, 15], the liver imaging parameters of PET/CT images can reflect the condition of the liver microenvironment, suggesting the possibility of a significant association between PET/CT parameter values and the risk of hepatic metastasis in patients with colorectal cancer. However, only a few studies have investigated the predictive value of CT-attenuation of the liver for hepatic metastasis and the prognostic significance of ^{18}F-FDG uptake in the liver has not yet been evaluated [7, 8].

Therefore, the present study aimed to investigate the prognostic value of CT-attenuation and ^{18}F-FDG uptake in the liver measured on ^{18}F-FDG PET/CT images for predicting hepatic recurrence after curative surgery in patients with colorectal cancer.

Subjects and Methods

Patients

The study was approved by the Institutional Review Board of Soonchunhyang University Cheonan Hospital and patient consent was waived due to the retrospective nature of the study. All procedures performed in the studies involving human participants were in accordance with the 1964 Helsinki Declaration and its later amendments.

We retrospectively reviewed the medical records of 388 patients who were histopathologically diagnosed with colorectal cancer and underwent ^{18}F-FDG PET/CT for a staging work-up between February 2012 and December 2018. Among them, we finally recruited 257 colorectal cancer patients who showed no distant metastasis, including hepatic metastases, on staging imaging examination, and subsequently underwent curative surgical resection. Patients who: 1) underwent neoadjuvant treatment before surgery, 2) underwent palliative surgery, 3) had a contrast-enhanced CT scan within 24 hours before the ^{18}F-FDG PET/CT scan (the contrast medium is likely to affect the measurement of the liver CT parameters), 4) had a history of chronic liver disease or another malignant disease, or 5) were lost to follow-up within 24 months after surgery without any event were excluded. Furthermore, one patient who had a rare pathological type of colon cancer (medullary carcinoma) was also excluded from the statistical analysis. For the staging work-up, all patients underwent colonoscopy, high-resolution noncontrast-enhanced chest CT, contrast-enhanced abdominopelvic CT, ^{18}F-FDG PET/CT, and blood tests including serum CEA, complete blood count, fasting glucose level, and routine liver biochemistry. The body mass index (BMI) was calculated from the weight and height measured at the time of the staging work-up for each patient, and obesity was defined as a BMI of >25kg/m^2. Using the results of the blood tests, the non-alcoholic fatty liver disease fibrosis score (NFS) was calculated [10]. Patients with an NFS of >0.676 were categorized as the high NFS group, and the other patients were categorized as the low NFS group [10]. After the staging work-up, curative surgical resection with regional lymph node dissection was performed and the pathologic T and N stages were evaluated. The histologic grade of the cancer lesions was assessed using a two-grade system of low-grade (well and moderately differentiated) and high-grade (poorly differentiated, mucinous, and undifferentiated) tumors. After surgery, all enrolled patients were regularly followed up with physical examinations, blood tests, and imaging studies. The patients with cancer recurrence were classified into two groups, those who showed hepatic recurrence irrespective of the presence of extrahepatic recurrence and those who showed only extrahepatic recurrence.

^{18}F-FDG PET/CT scan and image analysis

Fluorine-18-FDG PET/CT scans of all enrolled patients were performed using a Biograph mCT 128 scanner (Siemens Healthineers, Knoxville, TN, USA). All patients were instructed to fast at least six hours before PET/CT scanning. After confirming blood glucose levels of less than 200mg/dL, ^{18}F-FDG was intravenously injected at a dose of approximately 4.07 MBq/kg. Fluorine-18-FDG PET/CT scanning was performed 60 minutes after the injection from the skull base to the proximal thigh. A noncontrast-enhanced CT scan was initially performed at 100mA and 120kVp with a slice thickness of 5 mm, then a PET scan was performed at 1.5 minutes per bed position in a three-dimensional mode. Positron emission tomography images were reconstructed with a point-spread-function based Gauss and All pass filter algorithm and time-of-flight reconstruction with attenuation correction using the CT images.

Two nuclear medicine physicians measured the PET and CT parameters with blinding to the clinicopathologic factors and clinical outcomes of the patients. First, ^{18}F-FDG uptake in the primary colorectal cancer was measured by drawing a spheroid-shaped volume of interest (VOI) over the primary tumor lesion, and the maximum standardized uptake value (SUV) was calculated. Afterward, the mean CT-attenuation values of the liver and spleen were measured in Hounsfield units (HU) according to the method in a previous study [16]. Three regions of interest (ROI) in the liver and two ROI in the spleen, with an area of at least 100mm^2, were manually drawn in a single-slice of the CT image, avoiding vessels, focal lesions, and surface margins in the ROI, and the mean HU values of the liver and spleen were measured (Figure 1) [16]. For the PET parameters of the liver, the maximum and mean SUV was calculated using the three ROI used for the CT-attenuation measurement. Using the mean HU of the liver and spleen, the liver-spleen ratio (dividing the liver CT-attenuation by the spleen CT-attenuation) and the liver-spleen difference (subtracting the spleen CT-attenuation from the liver CT-attenuation) of the CT-attenuation were calculated. Therefore, a total of five parameters of the liver, three CT-attenuation parameters (liver HU, liver-spleen ratio, and liver-spleen difference) and two PET parameters (maximum and mean SUV of the liver), were measured in the PET/CT images.

Statistical analysis

To analyze the correlation between the liver CT-attenuation parameters and the clinicopathologic factors, the patients were dichotomized according to the liver CT-attenuation

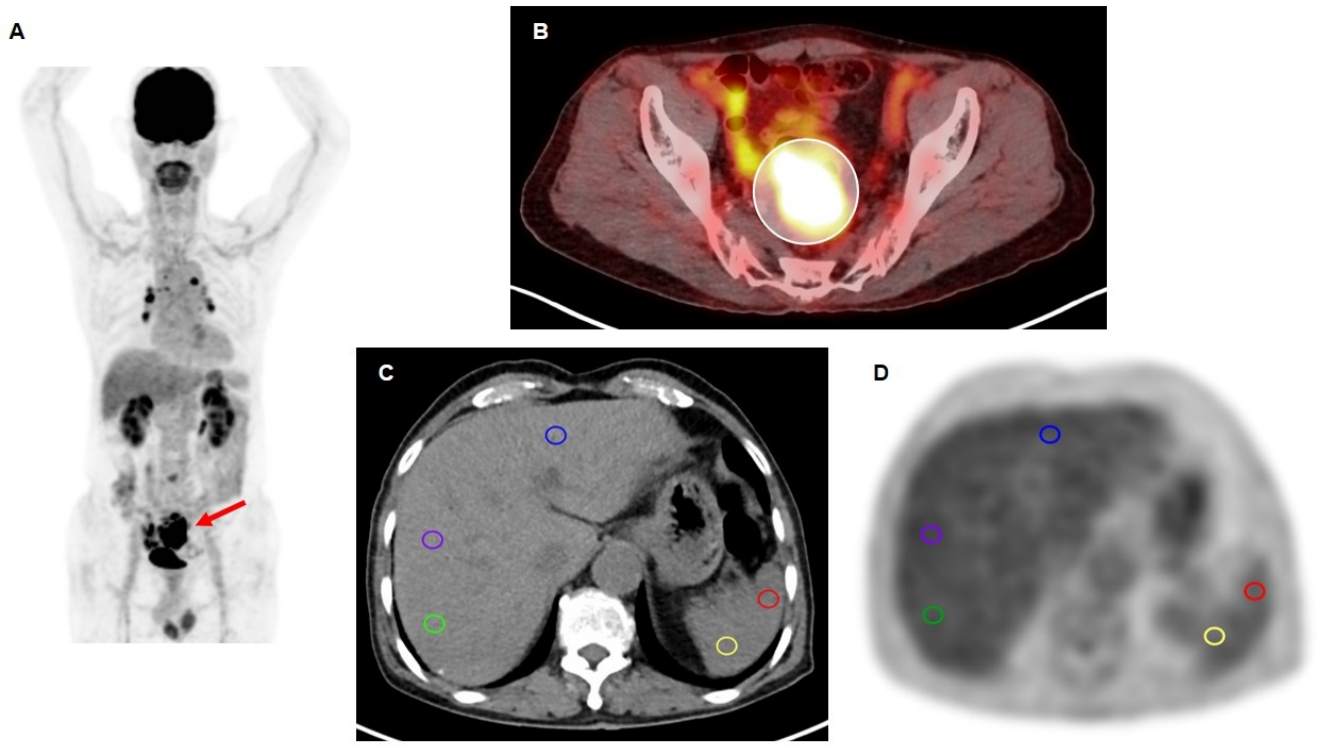

Figure 1. Measurement example of CT-attenuation and ^{18}F-FDG uptake in the liver. A 75-year-old man underwent ^{18}F-FDG PET/CT for the staging work-up of sigmoid colon cancer. In the maximal intensity projection image (A), the primary tumor lesion shows intensely increased ^{18}F-FDG uptake (arrow). In the transaxial images (B), a spheroid-shaped VOI was drawn over the primary tumor lesion, and the maximum SUV of the primary cancer lesion was measured. For calculating the CT-attenuation parameters of the liver, three ROI in the liver (blue, violet, and green circles) and two ROI in the spleen (red and yellow circles) with an area of at least 100mm^2 were manually drawn in a single-slice of the CT image (C), and the mean CT-attenuation values of the ROI were measured. For calculating the PET parameters of the liver, all ROI on the CT image were exported to the corresponding PET image, and the maximum and mean SUV of the three ROI in the liver were measured (D).

criteria for diagnosing hepatic steatosis that were established in previous studies (liver HU, 40HU; liver-spleen ratio, 1.10; liver-spleen difference, 5HU) [8, 14, 17]. Afterward, the chi-squared test and Fisher's exact test were performed to evaluate the differences in the proportion of patients. The Student's t-test and the Mann-Whitney U test were performed to evaluate the differences in continuous variables between the patient groups classified by the liver CT-attenuation criteria. The Student's t-test and the Mann-Whitney U test were performed to evaluate the differences in the liver PET parameter values between the patient groups. Spearman's correlation coefficients were calculated to assess the relationship between the PET parameters and continuous variables after evaluating the normality of the distribution by the Shapiro-Wilk test. For survival analysis, all continuous variables other than the liver CT-attenuation parameters were categorized into two groups according to the optimal cut-off values determined by the maximal chi-squared method. The significance of prognostic values of variables in the univariate and multivariate analyses for predicting recurrence-free survival (RFS), hepatic RFS, and extrahepatic RFS was assessed using the Cox proportional hazard regression test. Survival time was defined as the time from the day of curative surgery to the day of recurrence detection or the day of the last visit. In multivariate survival analysis, the predictive value of the liver CT-attenuation and PET parameters was assessed in four different models along with the TNM stage after adjusting for age, sex, and obesity. Survival curves of the variables were estimated using the Kaplan-Meier method to calculate the cumulative hepatic RFS. The ability of the combination of the TNM stage and liver parameters to predict hepatic RFS was assessed by calculating the Harrell concordance index (C-index). Statistical analyses were performed using R software version 3.6.3 (The R Foundation for Statistical Computing, Vienna, Austria) and MedCalc Statistical Software version 20 (MedCalc Software Ltd, Ostend, Belgium). A P-value of <0.05 was considered statistically significant.

Results

Clinicopathologic characteristics of the patients

The clinicopathologic features of the 257 enrolled patients with colorectal cancer are shown in Table 1. All enrolled patients were diagnosed with adenocarcinoma of the colon and rectum. Using established liver CT-attenuation criteria for diagnosing hepatic steatosis, hepatic steatosis was diagnosed in 18 patients (7.0%) by the liver HU criterion (liver HU ≤40HU), 64 patients (24.9%) by the liver-spleen ratio cri-

Table 1. *Clinicopathologic characteristics of the patients (n=257).*

Characteristics	Number of patients (%)		Median (range)
Age (years)			66 (26-88)
Sex	Men	143 (55.6%)	
	Women	114 (44.4%)	
Obesity (BMI >25 kg/m^2)	Absent	184 (71.6%)	
	Present	73 (28.4%)	
Diabetes mellitus	Absent	167 (65.0%)	
	Present	90 (35.0%)	
Location	Cecum and ascending colon	73 (28.4%)	
	Transverse and descending colon	28 (10.9%)	
	Sigmoid colon	124 (48.2%)	
	Rectum	29 (11.3%)	
	Multiple cancers	3 (1.2%)	
T stage	T1	19 (7.4%)	
	T2	34 (13.2%)	
	T3	156 (60.7%)	
	T4	48 (18.7%)	
Lymph node metastasis	Absent	156 (60.7%)	
	Present	101 (39.3%)	
TNM stage	Stage I	38 (14.8%)	
	Stage II	117 (45.5%)	
	Stage III	102 (39.6%)	
Tumor grade	Low	230 (89.5%)	
	High	27 (10.5%)	
Lymphatic invasion	Absent	172 (66.9%)	
	Present	85 (33.1%)	
Perineural invasion	Absent	191 (74.3%)	
	Present	66 (25.7%)	
Serum CEA (ng/mL)			3.7 (0.4-840.6)
NFS	Low	236 (91.8%)	
	High	21 (8.2%)	
CT	Liver HU (HU)		51.8 (28.2-71.5)
	Liver-spleen ratio		1.23 (0.74-3.44)
	Liver-spleen difference (HU)		9.5 (-12.0-36.8)
PET	Maximum tumor SUV		12.17 (2.65-49.90)
	Maximum liver SUV		2.52 (1.36-3.83)
	Mean liver SUV		2.06 (1.07-3.22)
Adjuvant treatment	No	70 (27.2%)	
	Chemotherapy	186 (72.4%)	
-	Chemoradio-therapy	1 (0.4%)	

BMI, body mass index; CEA, carcinoembryonic antigen; HU, Hounsfield unit; NFS, non-alcoholic fatty liver disease fibrosis score; SD, standard deviation; SUV, standardized uptake value

terion (liver-spleen ratio ≤1.10), and 67 patients (26.1%) by the liver-spleen difference criterion (liver-spleen difference <5HU). The median clinical follow-up duration was 50.2 months (range, 3.5-100.1 months). During the clinical follow-up, 54 patients (21.0%) experienced a cancer recurrence. Of these patients, hepatic recurrence was found in 22 patients (8.6%), comprised of 16 patients (6.2%) with only hepatic recurrence and six patients (2.3%) with both hepatic and extra-hepatic recurrences.

In the correlation analysis between the CT-attenuation and PET parameters of the liver, the maximum and mean SUV of the liver was significantly higher in patients with a low liver-spleen ratio and liver-spleen difference than those with high values (P<0.05; Table 2). The differences in the maximum and mean SUV of the liver were more obvious between the patients grouped by the liver-spleen ratio than by liver-spleen difference. Obesity was significantly associated with the liver CT-attenuation parameters (Table 2) and liver PET parameters (Table 3), showing higher proportions of patients with obesity in patients with low CT-attenuation parameter values and high PET parameter values. Diabetes mellitus also showed significant association with the liver CT-attenuation parameters and NFS revealed a significant relationship only with liver HU. All other clinicopathologic factors showed no significant correlation with the liver CT-attenuation parameters and liver PET parameters.

Table 2. *Relationship of liver CT-attenuation parameters with PET parameters and clinicopathologic factors.*

Factors		Liver HU		Liver-spleen ratio		Liver-spleen difference	
		≤40	>40	≤1.10	>1.10	<5	≥5
No. of patients (%)		18 (7.0%)	239 (93.0%)	64 (24.9%)	193 (75.1%)	67 (26.1%)	190 (73.9%)
Age*		64±9	65±13	65±11	64±13	65±11	64±13
	P-value		0.831		0.530		0.776
Sex	Men	7 (38.9%)	107 (44.8%)	21 (32.8%)	93 (48.2%)	21 (31.3%)	93 (48.9%)
	Women	11 (61.1%)	132 (55.2%)	43 (67.2%)	100 (51.8%)	46 (68.7%)	97 (51.1%)
	P-value		0.629		0.032		0.013
Obesity	Absent	8 (44.4%)	176 (73.6%)	38 (59.4%)	146 (75.6%)	39 (58.2%)	145 (76.3%)
	Present	10 (55.6%)	63 (26.4%)	26 (40.6%)	47 (24.4%)	28 (41.8%)	45 (23.7%)
	P-value		0.008		0.013		0.005
Diabetes mellitus	Absent	6 (33.3%)	161 (67.4%)	32 (50.0%)	135 (70.0%)	34 (50.7%)	133 (70.0%)
	Present	12 (66.7%)	78 (32.6%)	32 (50.0%)	58 (30.0%)	33 (49.3%)	57 (30.0%)
	P-value		0.004		0.004		0.005
TNM stage	Stage I-II	12 (66.7%)	143 (59.8%)	43 (67.2%)	112 (58.0%)	44 (65.7%)	111 (58.4%)
	Stage III	6 (33.3%)	96 (40.2%)	21 (32.8%)	81 (42.0%)	23 (34.3%)	79 (41.6%)
	P-value		0.568		0.195		0.300
Tumor grade	Low	16 (88.9%)	214 (89.5%)	56 (87.5%)	174 (90.2%)	58 (86.6%)	172 (90.5%)
	High	2 (11.1%)	25 (10.5%)	8 (12.5%)	19 (9.8%)	9 (13.4%)	18 (9.5%)
	P-value		0.931		0.549		0.364
Serum CEA*		5.4±4.0	11.9±56.0	6.3±7.9	13.1±62.1	6.2±7.8	13.2±62.6
	P-value		0.086		0.137		0.132
NFS	Low	14 (77.8%)	222 (92.9%)	56 (87.5%)	180 (93.3%)	59 (88.1%)	177 (93.2%)
	High	4 (22.2%)	17 (7.1%)	8 (12.5%)	13 (6.7%)	8 (11.9%)	13 (6.8%)
	P-value		0.024		0.145		0.191

(continued)

Maximum tumor SUV*		14.28±11.21	14.21±8.05	14.21±9.38	14.2±7.90	13.96±9.28	14.30±7.92
	P-value		0.977		0.996		0.789
Maximum liver SUV*		2.63 ± 0.53	2.52 ± 0.38	2.69 ± 0.42	2.48 ± 0.37	2.67 ± 0.42	2.49 ± 0.37
	P-value		0.415		<0.001		0.033
Mean liver SUV*		2.12±0.41	2.08±0.33	2.23±0.35	2.03±0.31	2.17±0.35	2.05±0.31
	P-value		0.671		<0.001		0.042

**Expressed in mean ± standard deviation*
CEA, carcinoembryonic antigen; HU, Hounsfield unit; NFS, non-alcoholic fatty liver disease fibrosis score; SUV, standardized uptake value

Table 3. *Relationship between PET parameters and clinicopathologic factors.*

Factors		Maximum liver SUV	Mean liver SUV
Age	Correlation coefficient	0.005	0.045
	P-value	0.935	0.469
Sex*	Men	2.56±0.42	2.07±0.35
	Women	2.50±0.35	2.09±0.31
	P-value	0.225	0.587
Obesity*	Absent	2.47±0.38	2.04±0.33
	Present	2.69±0.39	2.19±0.32
	P-value	<0.001	<0.001
Diabetes mellitus*	Absent	2.49 ± 0.40	2.04 ± 0.33
	Present	2.57 ± 0.39	2.11 ± 0.33
	P-value	0.200	0.197
TNM stage*	Stage I-II	2.55±0.39	2.10±0.33
	Stage III	2.50±0.41	2.05±0.34
	P-value	0.292	0.324
Tumor grade*	Low	2.53±0.39	2.08±0.33
	High	2.56±0.41	2.11±0.37
	P-value	0.668	0.694
Serum CEA	Correlation coefficient	-0.080	-0.080
	P-value	0.201	0.204
NFS*	Low	2.53±0.39	2.08±0.33
	High	2.57±0.49	2.13±0.40
	P-value	0.643	0.438

**Expressed in mean ± standard deviation*
CEA, carcinoembryonic antigen; NFS, non-alcoholic fatty liver disease fibrosis score; SUV, standardized uptake value

Survival analysis

The prognostic values of the five liver parameters as well as the clinicopathologic factors for predicting RFS, hepatic RFS, and extrahepatic RFS were assessed. For the liver CT-attenuation parameters, the established cut-off values for diagnosing hepatic steatosis were used for survival analysis. For the other continuous variables, the optimal cut-off values were selected by the maximal chi-squared method.

In the univariate analysis, liver-spleen ratio, liver-spleen difference, and the maximum SUV of the liver showed significant associations with RFS and hepatic RFS (P<0.05). Patients with a high liver-spleen ratio and liver-spleen differences had worse RFS and hepatic RFS than those with low values, whereas patients with a high maximum SUV of the liver showed better RFS and hepatic RFS than those with low vaues (Table 4; Figure2). The mean liver SUV showed a significant negative association only with hepatic RFS (P=0.022), and liver HU revealed no significant association with RFS or hepatic RFS (P>0.05). None of the liver parameters measured on PET/CT images revealed a significant association with extrahepatic RFS (P>0.05). Among the clinicopathologic factors, TNM stage and serum CEA level were significant predictors of RFS, hepatic RFS, and extrahepatic RFS (P<0.05; Table 4).

Table 4. *Univariate survival analysis for recurrence-free survival, hepatic recurrence-free survival, and extrahepatic recurrence-free survival.*

Variables	Recurrence-free survival		Hepatic recurrence-free survival		Extrahepatic recurrence-free survival	
	P-value	Hazard ratio (95% CI)	P-value	Hazard ratio (95% CI)	P-value	Hazard ratio (95% CI)
Age (≤65y vs. >65y)	0.109	0.64 (0.37-1.10)	0.126	0.51 (0.21-1.21)	0.321	0.72 (0.38-1.37)
Sex (women vs. men)	0.851	0.95 (0.55-1.63)	0.131	2.06 (0.81-5.28)	0.214	0.67 (0.35-1.26)
Obesity (absent vs. present)	0.133	0.60 (0.31-1.17)	0.807	1.12 (0.45-2.75)	0.154	0.55 (0.24-1.25)
TNM stage (I-II vs. III)	<0.001	3.45 (1.97-6.03)	0.002	4.55 (1.78-11.65)	0.002	2.84 (1.48-5.45)
Tumor grade (low vs. High)	0.722	0.85 (0.34-2.12)	0.388	0.41 (0.06-3.07)	0.753	0.97 (0.44-2.73)
Maximum tumor SUV (≤12.09 vs. >12.09)	0.650	1.13 (0.66-1.93)	0.308	1.27 (0.78-2.02)	0.284	0.70 (0.37-1.33)
Serum CEA (≤12.5ng/mL vs. >12.5ng/mL)	0.002	2.68 (1.44-5.02)	0.006	3.54 (1.44-8.72)	0.037	2.30 (1.05-5.04)
NFS (low vs. high)	0.123	0.43 (0.16-1.13)	0.201	0.88 (0.49-1.43)	0.262	0.32 (0.04-2.34)
Liver HU (≤40HU vs. >40HU)	0.581	1.39 (0.43-4.45)	0.602	1.71 (0.23-12.68)	0.573	1.51 (0.36-6.26)
Liver-spleen ratio (≤1.10 vs. >1.10)	0.037	2.23 (1.05-4.74)	0.014	3.22 (1.26-8.23)	0.208	1.70 (0.75-3.86)
Liver-spleen difference (<5 HU vs. ≥5 HU)	0.025	2.36 (1.11-5.02)	0.011	3.31 (1.31-8.34)	0.205	1.79 (0.79-4.07)
Maximum liver SUV (≤2.45 vs. >2.45)	0.039	0.51 (0.25-0.95)	0.006	0.27 (0.10-0.69)	0.270	0.70 (0.37-1.32)
Mean liver SUV (≤2.11 vs. >2.11)	0.276	0.73 (0.42-1.28)	0.022	0.28 (0.09-0.84)	0.717	1.01 (0.53-1.93)

CEA, carcinoembryonic antigen; CI, confidence interval; HU, Hounsfield unit; NFS, non-alcoholic fatty liver disease fibrosis score; SUV, standardized uptake value

Multivariate survival analysis for predicting hepatic RFS was performed with the TNM stage and the four liver parameters that showed statistical significance in the univariate analysis after adjusting for age, sex, and obesity (Table 5). Because of the significant correlations between the liver-spleen ratio and liver-spleen difference and between the maximum and mean liver SUV (P<0.001 and correlation coefficient of >0.500 for both), the prognostic values of the liver parameters were assessed in four separate models to minimized the effect of collinearity between the variables. In the multivariate analysis, the liver-spleen ratio, liver-spleen difference, and maximum SUV of the liver remained significant predictors of hepatic RFS (P<0.05). However, the mean liver SUV failed to show a significant predictive value (P>0.05).

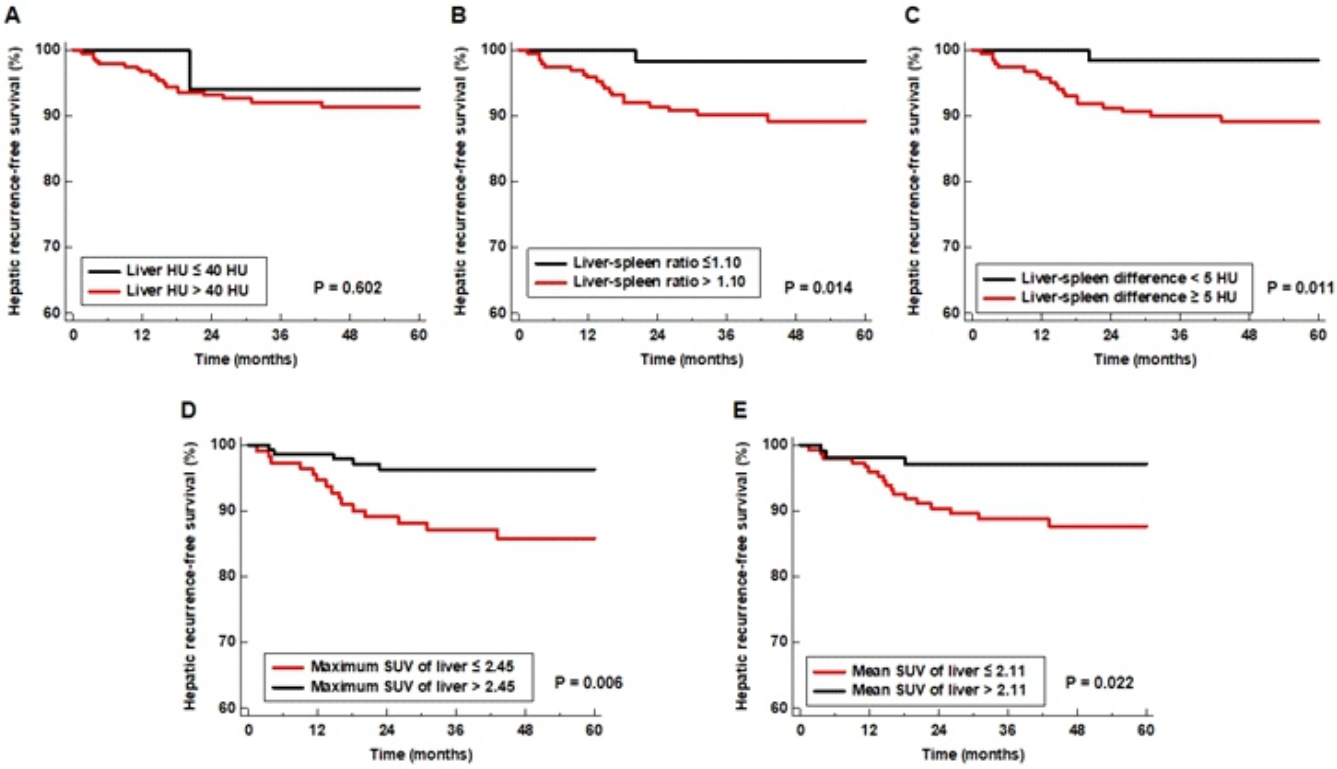

Figure 2. Kaplan-Meier survival curves for hepatic recurrence-free survival stratified by liver HU (A), liver-spleen ratio (B), liver-spleen difference (C), maximum liver SUV (D), and mean liver SUV (E).

Table 5. *Multivariate survival analysis for hepatic recurrence-free survival after adjusting for age, sex, and obesity.*

Variables	Model 1		Model 2		Model 3		Model 4	
	P-value	Hazard ratio (95% CI)	P-value	Hazard ratio (95% CI)	P-value	Hazard ratio (95% CI)	P-value	Hazard ratio (95% CI)
TNM stage	0.002	4.48 (1.72-11.64)	0.001	4.82 (1.87-12.42)	0.002	4.68 (1.80-12.19)	<0.001	5.22 (2.02-13.53)
Liver-spleen ratio	0.025	10.44 (1.35-80.92)	0.043	8.13 (1.07-62.04)	-	-	-	-
Liver-spleen difference	-	-	-	-	0.016	11.86 (1.53-82.06)	0.017	11.83 (1.51-92.98)
Maximum liver SUV	0.036	0.36 (0.14-0.94)	-	-	0.042	0.37 (0.14-0.96)	-	-
Mean liver SUV	-	-	0.133	0.43 (0.14-1.30)	-	-	0.098	0.38 (0.11-1.18)

CI, confidence interval; SUV, standardized uptake value

Hepatic RFS according to TNM stage and liver-spleen difference

We further compared the hepatic RFS of the enrolled patients according to the combination of TNM stage (stage I-II vs. stage III) and liver-spleen difference (<5 HU vs. ≥5 HU). There was a significant difference in hepatic RFS among the four patient groups stratified by TNM stage and liver-spleen difference (P< 0.001; Figure 3). Patients with TNM stage III and liver-spleen difference of ≥5HU had significantly worse hepatic RFS than those with TNM stage I-II and liver-spleen difference of <5HU (P=0.004; hazard ratio=4.06; 95% confidence interval (CI), 1.58-10.48), whereas there were no significant differences in hepatic RFS in the other three groups (P>0.05). Patients with stage III and liver-spleen difference of ≥5 HU had the worst 5-year hepatic RFS rate at 80.9%, whereas the 5-year hepatic RFS rate was 100.0% in patients with stage I-II and liver-spleen difference of <5HU, 94.8% in stage I-II and liver-spleen difference of ≥5HU, and 95.5% in stage III and liver-spleen difference of <5HU. In Harrell's C statistical analysis, the combination of the TNM stage and the liver-spleen difference demonstrated great discriminative ability in predicting hepatic RFS (C-index, 0.737; 95% CI, 0.679-0.790).

Discussion

Colorectal cancer is notable for its surprisingly high frequency of distant metastasis to a specific target organ, the liver [18]. The "seed and soil" hypothesis has been proposed to account for this specificity, suggesting that the permissive microenvironment of the liver (soil) is also crucial to the formation and growth of hepatic metastasis, as well as the biological characteristics of colorectal cancer cells (seed) [11, 18, 19]. Therefore, it is reasonable to assume that changes in the liver microenvironment can have a significant impact on the success of cancer cell implantation in either a favorable or adverse way [9]. Among the previous studies with animal models, some studies showed that fatty changes in the liver suppressed the formation of hepatic metastasis, while contrastingly, other studies revealed that hepatic steatosis could be beneficial to the growth of hepatic metastases[9, 20, 21]. These contradictory results were also seen in previous clinical studies with colorectal cancer patients. In previous studies, hepatic metastasis was found to be less frequent in patients with a fatty liver, and a prospective study demonstrated that hepatic steatosis significantly improved 5-year cancer-specific survival even after adjustment for other known prognostic factors [8, 22, 23]. In contrast, other studies reported that hepatic steatosis was more common in patients with hepatic metastasis, and patients with hepatic steatosis had a greater risk of hepatic recurrence than others [10, 24, 25]. Meanwhile, another two clinical studies failed to show either a positive or negative association between hepatic steatosis and the hepatic recurrence of colorectal cancer [26, 27]. These conflicting results are considered to result from different degrees of liver fatty changes in the enrolled patients and the various tools used to define hepatic steatosis including imaging modalities, blood tests, and biopsies [9].

In the present study, similar to the results of a previous study that used CT images for diagnosing hepatic steatosis [8], colorectal cancer patients with low liver CT-attenuation parameter values showed better hepatic RFS after curative surgery of the primary tumor than those with high values, implying that fatty changes in the liver provided an unfavorable microenvironment for the formation of hepatic metastasis. Taking into account the prognostic stratification by combining the tumor stage and liver-spleen difference, our

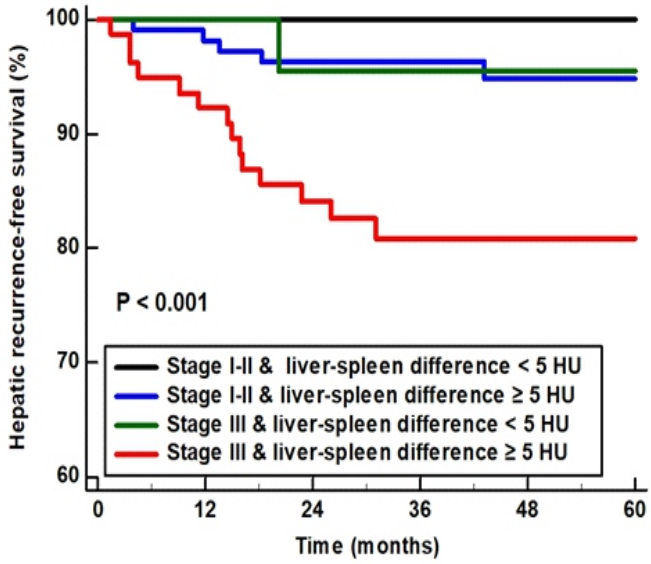

Figure 3. Hepatic recurrence-free survival stratified by the combination of TNM stage (stage I-II vs. stage III) and liver-spleen difference (<5HU vs. ≥5HU).

results suggest that both the seed (tumor stage) and soil (liver-spleen difference) factors were essential for the development of hepatic metastasis. In the literature, diverse CT-attenuation criteria have been used for diagnosing hepatic steatosis, and a wide range of hepatic steatosis prevalence from 6.2% using a liver HU of ≤40HU to 45.9% using a liver-spleen ratio of ≤1.10 has been reported [14, 16]. Hence, we measured three different CT-attenuation parameters of the liver and evaluated the prognostic value of each. The results of the survival analysis in our study revealed that both the liver-spleen ratio and the liver-spleen difference were significantly associated with hepatic RFS, whereas the liver HU was not a significant predictor of any survival outcome. Therefore, in our study, the liver-spleen ratio and the liver-spleen difference are suggested as optimal liver CT parameters for predicting hepatic RFS. However, due to the retrospective nature of the study, we could not assess the relationship between the liver CT parameters and histopathological findings of the liver to determine whether the liver-spleen ratio and the liver-spleen difference actually reflected the degree of fatty change in the liver better than the liver HU. Further studies are needed to investigate which liver CT parameter is the most suitable imaging parameter for reflecting the microenvironmental condition of the liver and to validate the results of the present study.

Our study also demonstrated that the maximum liver SUV was an independent predictor for hepatic RFS. For patients with malignant diseases, the liver has been often used as the reference organ for normalizing ^{18}F-FDG uptake in cancer lesions because of its stable ^{18}F-FDG uptake [28]. However, ^{18}F-FDG uptake of the liver is affected by multiple factors, which might limit the suitability of the liver as a reference organ [28]. In recent studies, ^{18}F-FDG uptake was positively correlated with microinflammatory lesions in the liver and the degree of liver fibrosis, suggesting the influence of liver inflammatory condition on ^{18}F-FDG uptake [15, 29]. These findings might be a possible explanation for our results. Although the biological mechanisms of the protective effect of hepatic steatosis on hepatic metastasis are not well known, enhanced local immune function through the activation of natural killer T cells by fat deposition in the liver has been proposed as one of the possible explanations for the relationship [8, 9]. Taking into consideration of the results in our study, decreased CT-attenuation parameter values and increased ^{18}F-FDG uptake in the liver might reflect a high degree of inflammatory status in the liver by fat deposition. This high-degree of inflammation could lead to enhanced anti-tumor immunity in the liver, which reduced hepatic recurrence risk [8, 30]. However, further studies are necessary to investigate the underlying mechanism.

Among the previous clinical studies regarding the relationship between hepatic steatosis and hepatic recurrence in colorectal cancer patients, all studies that used imaging modalities including CT for identifying hepatic steatosis showed a negative association between hepatic steatosis and hepatic metastasis [8, 22]. Non contrast-enhanced CT is known as a feasible and reproducible imaging modality for identifying fatty liver [14, 16]. However, significant discordances in the diagnosis of fatty liver disease were found between CT and other diagnostic tools including serum tests and liver biopsies, and, in our study, NFS, which is used to diagnose fatty liver disease and steatohepatitis, had no significant correlation with the liver PET/CT parameter values [9, 10]. Therefore, given that CT-attenuation and ^{18}F-FDG uptake can reflect the qualitative changes of the tissue microenvironment, there is a possibility that the PET/CT parameters of the liver might play a role as a stand-alone imaging biomarker of the liver microenvironmental condition for estimating the risk of hepatic metastasis of colorectal cancer, rather than as a simple tool for identifying hepatic steatosis.

The present study had several limitations. First, because the study was retrospectively performed with a relatively small number of patients enrolled from a single medical center, there might have been an inherent risk of selection bias. Second, because different stages of hepatic steatosis might have different effects on hepatic metastasis [8, 9], the results of our study should be validated in other populations. Third, further studies with the histopathological and immunological results from liver tissue biopsies are needed to prove the negative association between PET/CT parameters of the liver and hepatic RFS. Fourth, hepatic diseases other than viral and alcoholic liver diseases might be present in the enrolled patients and affect the results. Finally, since fatty liver disease and steatohepatitis are potentially reversible disease conditions, the micro-environmental condition of the liver might be changed during the follow-up period.

In conclusion, CT-attenuation parameters and maximum ^{18}F-FDG uptake in the liver measured on ^{18}F-FDG PET/CT were independently associated with hepatic RFS. The patients with a low liver-spleen ratio and liver-spleen differences and a high maximum SUV of liver showed better hepatic RFS than those with a high liver-spleen ratio and liver-spleen difference and a low maximum SUV of liver. These results suggest that imaging parameters of the liver on ^{18}F-FDG PET/CT could be used as imaging biomarkers that reflect the condition of the liver and predict the risk of hepatic metastasis in patients with colorectal cancer.

Acknowledgements

This study was supported by the National Research Foundation of Korea (NRF) grant funded by the Korean government (Ministry of Science and ICT) (grant number: 2022R1-C1C1002705) and by Soonchunhyang University Research Fund. The funders had no role in the design of the study; in the collection, analyses, or interpretation of data; in the writing of the manuscript, or in the decision to publish the results.

The authors declare that they have no conflicts of interest.

Bibliography

1. McMillan DC, McArdle CS. Epidemiology of colorectal liver metastases. *Surg Oncol* 2007; 16: 3-5.
2. Dörr NM, Bartels M, Morgul MH. Current treatment of colorectal liver metastasis as a chronic disease. *Anticancer Res* 2020; 40: 1-7.
3. Assumpcao L, Choti MA, Gleisner AL et al. Patterns of recurrence following liver resection for colorectal metastases: effect of primary rectal tumor site. *Arch Surg* 2008; 143: 743-9.

4. Ma ZH, Wang YP, Zheng WH, Ma J, Bai X, Zhang Y et al. Prognostic factors and therapeutic effects of different treatment modalities for colorectal cancer liver metastases. *World J Gastrointest Oncol* 2020; 12: 1177-94.
5. Ghiringhelli F, Hennequin A, Drouillard A et al. Epidemiology and prognosis of synchronous and metachronous colon cancer metastases: a French population-based study. *Dig Liver Dis* 2014; 46: 854-8.
6. Yang G, Wang G, Sun J et al. The prognosis of radiofrequency ablation versus hepatic resection for patients with colorectal liver metastases: A systematic review and meta-analysis based on 22 studies. *Int J Surg* 2021; 87:105896.
7. Lee S, Choe EK, Kim SY et al. Liver imaging features by convolutional neural network to predict the metachronous liver metastasis in stage I-III colorectal cancer patients based on preoperative abdominal CT scan. *BMC Bioinformatics* 2020; 21: 382.
8. Murono K, Kitayama J, Tsuno NH et al. Hepatic steatosis is associated with lower incidence of liver metastasis from colorectal cancer. *Int J Colorectal Dis* 2013; 28: 1065-72.
9. Lv Y, Patel N, Zhang HJ. The progress of non-alcoholic fatty liver disease as the risk of liver metastasis in colorectal cancer. *Expert Rev Gastroenterol Hepatol* 2019; 13: 1169-80.
10. Kondo T, Okabayashi K, Hasegawa H et al. The impact of hepatic fibrosis on the incidence of liver metastasis from colorectal cancer. *Br J Cancer* 2016; 115: 34-9.
11. Liu Q, Zhang H, Jiang X et al. Factors involved in cancer metastasis: a better understanding to "seed and soil" hypothesis. *Mol Cancer* 2017; 16: 176.
12. Lee JY, Yoon SM, Kim JT et al. Diagnostic and prognostic value of preoperative ^{18}F-fluorodeoxyglucose positron emission tomography/computed tomography for colorectal cancer: comparison with conventional computed tomography. *Intest Res* 2017; 15: 208-14.
13. Lee JW, Baek MJ, Ahn TS et al. Fluorine-18-fluorodeoxyglucose uptake of bone marrow on PET/CT can predict prognosis in patients with colorectal cancer after curative surgical resection. *Eur J Gastroenterol Hepatol* 2018; 30: 187-94.
14. Boyce CJ, Pickhardt PJ, Kim DH et al. Hepatic steatosis (fatty liver disease) in asymptomatic adults identified by unenhanced low-dose CT. *Am J Roentgenol* 2010; 194: 623-8.
15. Pak K, Kim SJ, Kim IJ et al. Hepatic ^{18}F-FDG uptake is not associated with hepatic steatosis but with visceral fat volume in cancer screening. *Nucl Med Mol Imaging* 2012; 46: 176-81.
16. Speliotes EK, Massaro JM, Hoffmann U et al. Liver fat is reproducibly measured using computed tomography in the Framingham Heart Study. *J Gastroenterol Hepatol* 2008; 23: 894-9.
17. Lee HJ, Lee CH, Kim S et al. Association between vascular inflammation and non-alcoholic fatty liver disease: Analysis by ^{18}F-fluorodeoxyglucose positron emission tomography. *Metabolism* 2017; 67: 72-9.
18. Kuo TH, Kubota T, Watanabe M et al. Liver colonization competence governs colon cancer metastasis. *Proc Natl Acad Sci USA* 1995; 92: 12085-9.
19. Seretis F, Seretis C, Youssef H et al. Colorectal cancer: seed and soil hypothesis revisited. *Anticancer Res* 2014; 34: 2087-94.
20. Karube H, Masuda H, Hayashi S et al. Fatty liver suppressed the angiogenesis in liver metastatic lesions. *Hepatogastroenterology* 2000; 47: 1541-5.
21. VanSaun MN, Lee IK, Washington MK et al. High fat diet induced hepatic steatosis establishes a permissive microenvironment for colorectal metastases and promotes primary dysplasia in a murine model. *Am J Pathol* 2009; 175: 355-64.
22. Hayashi S, Masuda H, Shigematsu M. Liver metastasis rare in colorectal cancer patients with fatty liver. *Hepatogastroenterology* 1997; 44: 1069-75.
23. Parkin E, O'Reilly DA, Adam R et al. The effect of hepatic steatosis on survival following resection of colorectal liver metastases in patients without preoperative chemotherapy. *HPB (Oxford)* 2013; 15: 463-72.
24. Hamady ZZ, Rees M, Welsh FK et al. Fatty liver disease as a predictor of local recurrence following resection of colorectal liver metastases. *Br J Surg* 2013; 100: 820-6.
25. Schulz PO, Ferreira FG, Nascimento Mde F et al. Association of nonalcoholic fatty liver disease and liver cancer. *World J Gastroenterol* 2015; 21: 913-8.
26. Ramos E, Torras J, Lladó L et al. The influence of steatosis on the short- and long-term results of resection of liver metastases from colorectal carcinoma. *HPB (Oxford)* 2016; 18: 389-96.
27. Molla NW, Hassanain MM, Fadel Z et al. Effect of non-alcoholic liver disease on recurrence rate and liver regeneration after liver resection for colorectal liver metastases. *Curr Oncol* 2017; 24: e233-e43.
28. Yoo ID, Lee SM, Lee JW et al. The influence of adipose tissue volume can significantly affect the metabolic activity of reference organs in ^{18}F-FDG PET/CT studies of a normal healthy population. *Hell J Nucl Med* 2017; 20: 211-6.
29. Verloh N, Einspieler I, Utpatel K et al. In vivo confirmation of altered hepatic glucose metabolism in patients with liver fibrosis/cirrhosis by ^{18}F-FDG PET/CT. *EJNMMI Res* 2018; 8: 98.
30. Keramida G, Peters AM. ^{18}F-FDG PET/CT of the non-malignant liver in an in-creasingly obese world population. *Clin Physiol Funct Imaging* 2020; 40: 304-19.